Identification of the Irreversible Redox Behavior of Highly Fluorescent Benzothiadiazoles

Philipp Rietsch[+],[a] Sebastian Sobottka[+],[b] Katrin Hoffmann,[c] Pascal Hildebrandt,[a] Biprajit Sarkar,[b, d] Ute Resch-Genger,*[c] and Siegfried Eigler*[a]

Redox switches are applied in various fields of research, including molecular lifts, electronic devices and sensors. Switching the absorbance between UV and Vis/NIR by redox processes is of interest for applications in light harvesting or biomedicine. Here, we present a series of push-pull benzothiadiazole derivatives with high fluorescence quantum yields in solution and in the crystalline solid state. Spectroelectrochemical analysis reveals the switching of UV-absorption in the neutral state to Vis/NIR absorption in the reduced state. We identify the partial irreversibility of the switching process, which appears to be reversible on the cyclic voltammetry timescale.

The class of benzothiadiazoles (BTD) bears tunable absorption and emission features. Hence, their bandgap and orbital energies can be adjusted making those fluorophores attractive for fundamental photophysical research. BTDs are synthetically accessible from *o*-phenylenediamine derivatives as starting materials. Subsequent coupling reactions like Sonogashira, Suzuki, and Buchwald-Hartwig coupling give access to a plethora of symmetrical and unsymmetrical derivatives.[1–4] BTDs can be applied in organic light-emitting diode (OLED) materials,[5–7] polymers with defined electronic and optical properties,[8–10] in sensory metal-organic frameworks,[11] solar cells[12] or in field-effect transistors (FET).[13] Furthermore, BTDs can act as *ortho*-diamine protecting groups and can thus be used as precursors for other molecular compounds, e.g. diaminodicyanoquinones and quinoxalines.[14,15] Although, those applications involve redox processes, there are few publications where the BTD unit was considered as a redox switch.[16] In this regard, most currently used redox switches are based on, e.g. organometallic motives or complex organic structures such as perylenediimide-dithienylethene dyads.[17–20]

Up to now, spectroelectrochemical properties of BTDs have been investigated in studies on p- and n-doping effects in deposited thin films.[21,22] However, there are no examples reported which focus on establishing potentially electrochromic switches using the BTD molecular unit. In this regard, cyclovoltammetry (CV)-experiments give evidence for the electrochemical reversibility of redox processes. However, here we show that spectroelectrochemical investigations give a more reliable proof of the chemical (ir)reversibility of redox processes. Accordingly, herein we present a series of push-pull BTD derivatives with an identical electron-donating alkyne-methoxy group on one side and a variation of (electron-withdrawing) groups on the other side (Figure 1). We furthermore analyzed the fluorosolvatochromism of these compounds and measured fluorescence decay kinetics/fluorescence lifetimes (τ) and fluorescence quantum yields in solution (Φ_{fl}) and solid state (Φ_{fl}^{SS}). We investigated the non-radiative relaxation through measurements in primary alcohols of different chain length and in mixtures of ethanol and polyethylene glycol 400 (EtOH/PEG), thereby separating the effect of viscosity and polarity on BTD emission.

We started the synthesis of the presented BTD derivatives from *o*-diaminobenzene and followed the published procedure (Figure 1).[1] Compounds **1**–**4** were synthesized according to procedures of Park *et al.*[23] Compounds **2** and **4** were isolated from the same reaction mixture in respective yields of 12% and 54%.

The photophysical characterization was subsequently done in four solvents of varying polarity and proticity, namely n-hexane (apolar and aprotic), dichloromethane (DCM; medium polarity, aprotic), dimethylsulfoxide (DMSO; polar and aprotic), and ethanol (EtOH; polar and protic). The absorption and fluorescence spectra of **1**–**4** in DCM are shown in Figure 1B. The molar extinction coefficients (ε) of **1**–**4** reach a maximum at about 300 nm with values up to 35,000 $M^{-1}cm^{-1}$ and show a second absorption maximum around 400 nm with smaller ε values of about 10,000 $M^{-1}cm^{-1}$. The smaller ε values in n-hexane and EtOH might arise either from solubility/aggregation issues, possibly in conjunction with the hydrogen bonding to

[a] P. Rietsch,[+] P. Hildebrandt, Prof. Dr. S. Eigler
Institute of Chemistry and Biochemistry
Freie Universität Berlin
Takustraße 3, 14195 Berlin (Germany)
E-mail: siegfried.eigler@fu-berlin.de
[b] Dr. S. Sobottka,[+] Prof. Dr. B. Sarkar
Institute of Chemistry and Biochemistry
Freie Universität Berlin
Fabeckstraße 34-36, 14195 Berlin (Germany)
[c] Dr. K. Hoffmann, Dr. U. Resch-Genger
Department 1, Division Biophotonics
Bundesanstalt für Materialforschung und -prüfung (BAM)
Richard Willstätter Straße 11, 12489 Berlin (Germany)
E-mail: ute.resch@bam.de
[d] Prof. Dr. B. Sarkar
Chair of Inorganic Coordination Chemistry
Institute of Inorganic Chemistry
University of Stuttgart
Pfaffenwaldring 55, 70569 Stuttgart (Germany)
[+] These authors contributed equally to this manuscript.

Supporting information for this article is available on the WWW under https://doi.org/10.1002/cptc.202000050

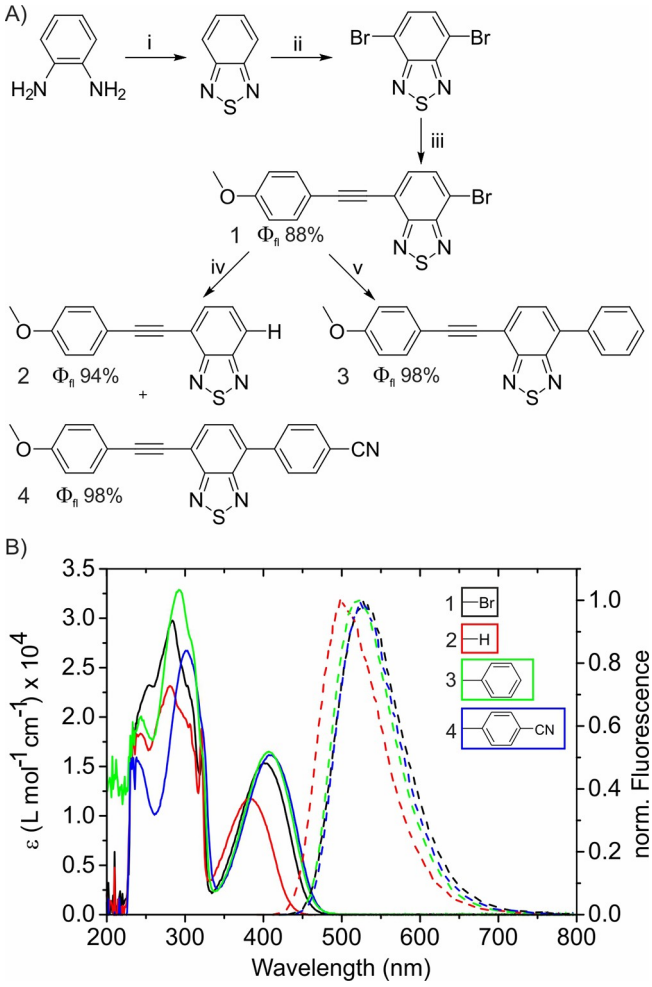

Figure 1. A) Synthetic route to benzothiadiazole derivatives **1**–**4**. i) $SOCl_2$, dichloromethane (DCM), 5 h, reflux; ii) HBr, Br_2; iii) THF, TEA, 1-ethynyl-4-methoxybenzene, $Pd(PPh_3)_2Cl_2$, CuI; iv) THF/H_2O, 1.2 eq. of the respective boronic acid, K_2CO_3, $Pd(PPh_3)_4$. Compounds **2** and **4** were isolated from the same reaction mixture in yields of 12% and 54%. v) THF/H_2O, 1.2 eq. phenyl boronic acid, K_2CO_3, $Pd(PPh_3)_4$, yield: 96%. The fluorescence quantum yields (Φ_{fl}) of **1**–**4** in DCM are given in %. B) Absorption spectra and normalized fluorescence spectra of **1**–**4** in DCM. The dye concentration was $10^{<M->5}$M.

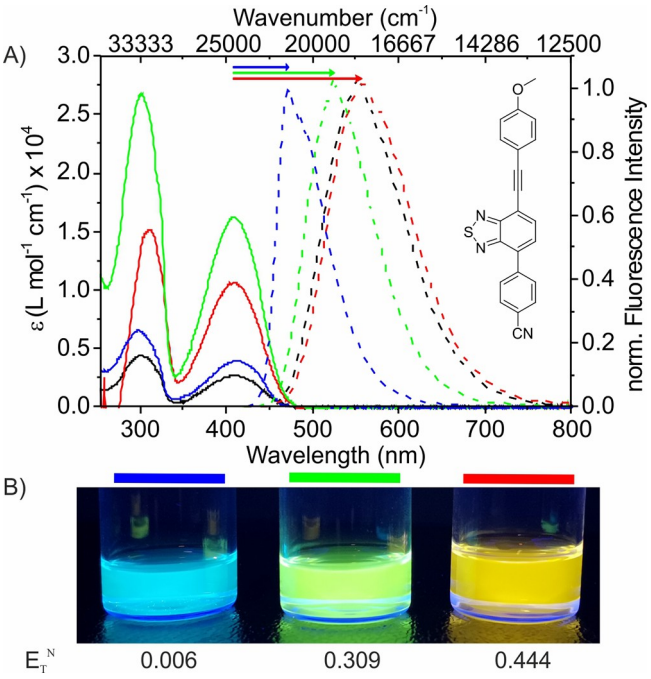

Figure 2. A) Absorption spectra (solid) and normalized fluorescence emission spectra (dashed, excitation at 410 nm) of **4** in solvents of different polarity. Hexane = blue, DCM = green, DMSO = red, EtOH = black. Arrows indicate the respective stokes shift. B) Solutions of **4** in solvents of the same proticity (aprotic) but different polarity (left to right: hexane, DCM, DMSO) under illumination with 366 nm. Values for the normalized Dimroth-Reichardt Parameter E_T^N were taken from Ref. [24]. The dye concentrations used for these measurements were $10^{<M->5}$M.

the nitrogen atom in the BTD core unit in case of EtOH. The high energy absorption band around 300 nm was attributed to π-π* transitions and the low energy absorption band to the HOMO-LUMO transition involving an intramolecular charge transfer (ICT) state.[25,26] To elucidate the role of the two absorption bands on dye emission, we measured an excitation emission matrix (EEM) of **3** in hexane (Figure S2), thereby demonstrating that excitation at both absorption maxima induce the same emission located at 473 nm.

Subsequently, we assessed the influence of solvent polarity and proticity on the emission properties of **1**–**4**. The red shift of the fluorescence maximum (Figure 2A) from 473 nm in hexane to 522 nm in DCM and 550 nm in DMSO of **4** is visible by the naked eye (Figure 2B).

The emission spectra in the polar aprotic and protic solvents DMSO and EtOH closely match. An increase in solvent polarity results also in a broadening of the emission band of **4**, the full width at half maximum (FWHM) of the gaussian fits of the fluorescence spectra decrease from 15×10^4 cm^{-1} in hexane to 0.9×10^4 cm^{-1} in ethanol (Table S2). Exemplary spectroscopic results of fluorosolvatochromism are shown in Figure 3, where **4** was analyzed in primary alcohols of different chain length, from EtOH ($E_T^N = 0.654$) to 1-decanol ($E_T^N = 0.525$). As the polarity of these alcohols changes only slightly compared to the other solvents (hexane, DCM, DMSO, EtOH), the solvatochromic shifts are smaller. The absorption band is red shifted with increasing polarity whereas the fluorescence maxima are blue shifted. The S_1-S_0 energy gap is thus decreasing. This effect is furthermore enhanced by the increasing refractive index of the alcohols with increasing chain length.[27] Solvent dependency of absorption and emission was investigated by Lippert and Mataga separately in the 1950s and later merged in the Lippert-Mataga equation [Eq. (S1)].

Although this model is built on simplified solvent-chromophore interactions and the assumption of a spherical chromophore (Onsager radius), it is widely used to describe solvatochromism and was used for BTDs before.[27–30] In Figure S7 the Lippert-Mataga plot of **1**–**4** is shown. The dipole change upon excitation is lowest for **1** (12.26 Debye) and highest for **4** (18 Debye). In addition, **4** also bears the highest ground state dipole moment as revealed by DFT calculations (Table S3). Both effects are ascribed to the cyano-group substituent. An increasing dipole moment upon excitation was found for BTDs before and is a well-known phenomenon.[24,30] To explain the

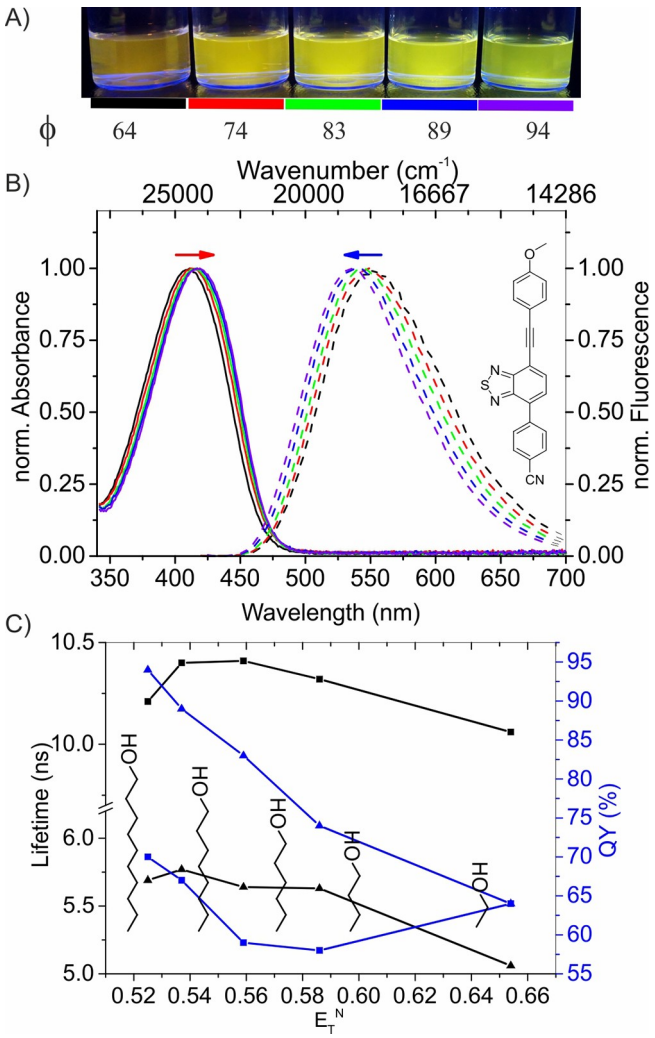

Figure 3. A) Photograph of solutions (10^{-5} M) of **4** in the alcohols ethanol (black), 1-butanol (red), 1-hexanol (green), 1-octanol (blue) and 1-decanol (purple) under illumination with 366 nm light. The respective quantum yields are indicated below in %. B) Normalized absorption spectra (solid lines) and emission spectra (dashed lines) of **4** (color code as in A). The Stokes shift decreases with increasing length of the alcohol chain and hence decreasing polarity. The red shift of the absorption and emission are marked by red and blue arrows, respectively. C) Fluorescence lifetime (black; right axis) and fluorescence quantum yield (blue; left axis) values in primary alcohols of decreasing chain length, revealing the polarity-induced changes of both features and their correlation. The concentrations of the measurements were $10^{<M->5}$M.

small difference in the change of the dipole moment for **4** in the two plots (aprotic solvents *vs.* series of primary alcohols in Figure S7), we measured **4** in EtOH-PEG mixtures containing increasing percentages of PEG400. There is almost no difference of the Dimroth-Reichardt polarity parameter E_T^N between PEG400 (0.66) and EtOH (0.65).[24,31] Thus, addition of PEG increases the viscosity drastically but changes the polarity only slightly (Figure S11).[32] We observe no shift in the absorption maximum and a small bathochromic shift of approx. 4 nm for the fluorescence maximum with increasing viscosity of the dye microenvironment. Thus, the polarity and the proticity of the alcohols seem to be responsible for the observed difference in the Lippert-Mataga plot.

We measured the Φ_{fl} and the fluorescence decay kinetics and therefore τ of the BDT dyes **1**–**4** in a series of solvents of increasing polarity and viscosity as well as in the solid state. The Φ_{fl} are consistently maximal in DCM, with values of 98% for **3** and **4**, thus reaching almost unity (Table 1). All compounds show the lowest Φ_{fl} in EtOH, the solvent with the highest polarity and highest hydrogen bonding strength.[33] Compounds **1** and **2** show a remarkably strong reduction of Φ_{fl} in EtOH (15% and 16%) and reduced τ of 4.12 ns (**1**) and 2.42 ns (**2**). This effect is ascribed to hydrogen bonding to the nitrogen atom of the BTD core, which is rather unprotected in **1** and **2** but sterically shielded by the phenyl substituents in **3** and **4**.

Furthermore, the formation of an ICT state in solvents of high polarity and emission from a locally excited (LE) state in solvents of low polarity, which was found to be dependent on the distance of the donor and acceptor moieties in push-pull systems, could explain the trend of the generally lower Φ_{fl} and τ in polar ethanol.[25,27,30,34] The highest τ values (Table S5) are found for **2** in DCM (10.02 ns) and DMSO (9.05 ns).

With increasing chain length of the solvent alcohol, and thus decreasing polarity, decreasing hydrogen bonding strength and increasing viscosity, τ and the Φ_{fl} of **4** increase (Figure 3C and Table S6). Accordingly, from ethanol to 1-decanol τ increases by 12.5% and Φ_{fl} by 47%. Since Φ_{fl} and τ increase with increasing viscosity are well known phenomena,[15,35,36] we compared our results with solutions of **4** in mixtures of EtOH-PEG with increasing viscosity but only slightly changing polarity (Figure S11). Here, both values increase as well, 1.2% for τ and 7.8% for Φ_{fl} (Table S7). As the viscosity in the EtOH/PEG mixtures and the series of alcohols is increasing, we conclude that the drastic reduction of solvent polarity from ethanol to 1-decanol is the reason for the 47% change of Φ_{fl}. This is in accordance with results published in 2014 by VanVeller *et al.*[3] and for other fluorophores with ICT character.[27]

Next, we measured the solid-state emission spectra (Figure 4 and Figure S14/S15) and Φ_{fl}^{SS} (Table 1, last row). As the mechanochromic nature of BTDs was shown before, all samples were ground before the spectroscopic measurements.[37] The solid state fluorescence spectra of our BDT dyes (Figure 4 and Figure S14/S15) closely match with the respective fluorescence spectra in DCM. The Φ_{fl}^{SS} are between 33% (**1**) and 72% (**3**) and are thus lower compared to the values determined in n-

Table 1. Fluorescence quantum yields of compounds **1**–**4** in solvents of different polarity. The values for the normalized Dimroth-Reichardt Parameter E_T^N were taken from Ref. [38]. The values for the orientation polarization Δf were calculated as described in detail in the Supporting Information.

E_T^N	Δf	Solvent	**1** Φ [%]	**2** Φ [%]	**3** Φ [%]	**4** Φ [%]
0.006	0.00	n-hexane	77	55	78	79
0.309	0.22	DCM	88	94	98	98
0.444	0.30	DMSO	58	83	78	87
0.654	0.29	EtOH	15	16	58	64
		Solid state	33	41	72	58

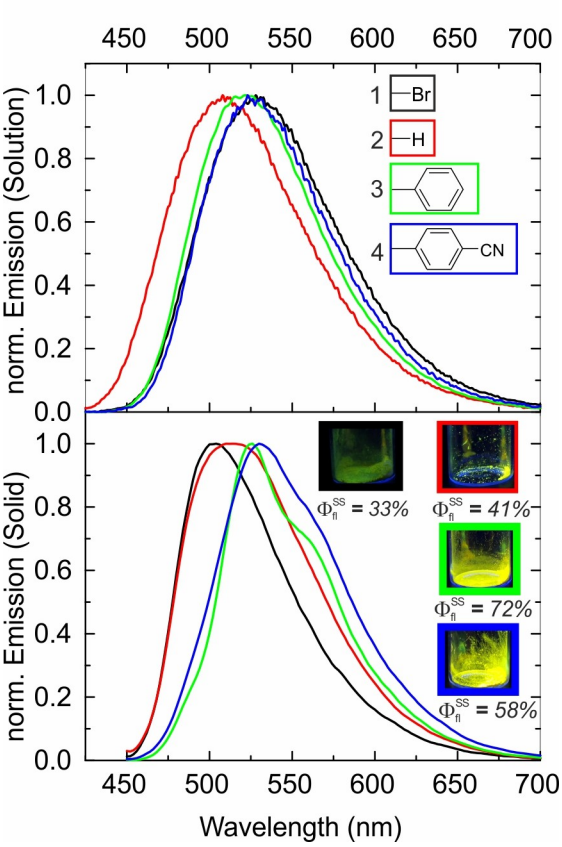

Figure 4. Normalized emission spectra of **1**–**4** in DCM (top, $10^{<M->5}$M) and in the solid-state (bottom). The insets show the molecular structure (top) with a color code used for the spectra and photographs of the crystal powders (bottom) under illumination with 366 nm light as well as the fluorescence quantum yields measured in the solid state (Φ_{fl}^{SS}).

hexane, DCM or DMSO, but higher compared to EtOH (exception: **4** with 64% *vs.* 58%) in the solid state.

Overall, **1** is the least emissive compound and **3** and **4** are the more fluorescent ones of this series in solution, particularly in polar solvents, as well as in the solid-state. Moreover, the Φ_{fl}^{SS} values observed in this study for solid **1**–**4** (Table 1) considerably exceed the Φ_{fl}^{SS} values published for BTDs so far, that are below 25%, even though these values were measured in spin-coated thin films.[2]

To gain more insights into the redox behavior of our BTD dyes we performed cyclic voltammetry (CV) as well as spectroelectrochemical (UV/Vis/NIR) measurements for **1**–**4** in a 0.1 M Bu_4NPF_6 solution of DCM (Figure 5 and S16–S18). The values of the electrochemical potentials are given relative to the ferrocene/ferrocenium couple (Fc/Fc^+). All compounds show at least one reduction process, which is electrochemically reversible for **2**–**4** with potentials around −1.75 V (Table S8).

The reduction of compound **1** is only partially reversible. Compounds **2** and **4** show another irreversible reductive process at −2.11 V and −2.23 V, respectively (Table S8). This is rather surprising, since BTDs are well known to expel the sulfur atom upon reduction.[14,39] However, the reduction of compound **1** most likely results in partial dehalogenation. All compounds show irreversible oxidation processes around

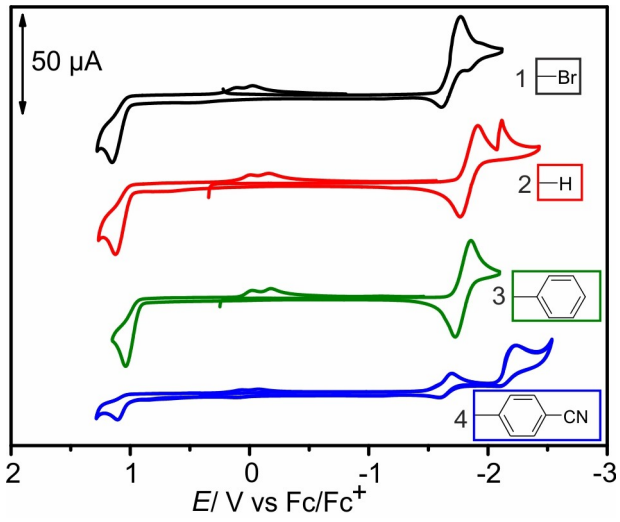

Figure 5. Cyclic voltammogram of **1**–**4** measured at 100 mV/s in 0.1 M Bu_4NPF_6 solution of DCM.

+1 V, which most likely induce a chemical reaction involving the alkyne moiety. This chemical reaction might be a ring-closure with the nitrogen atoms, as this seems to be a common feature in electrochemical reactions of similar compounds.[40] The resulting species show re-reduction processes at around 0 V for **1**–**4**. Scan direction-dependent measurements of **4** (starting with either oxidation or reduction first) indicate that these peaks are linked to the oxidation (Figure S18). The same observation holds true for **1**–**3**, if an appropriate starting potential is chosen. For compound **4**, the inset in Figure 6 confirms that the oxidation is crucial for the redox process at 0 V.

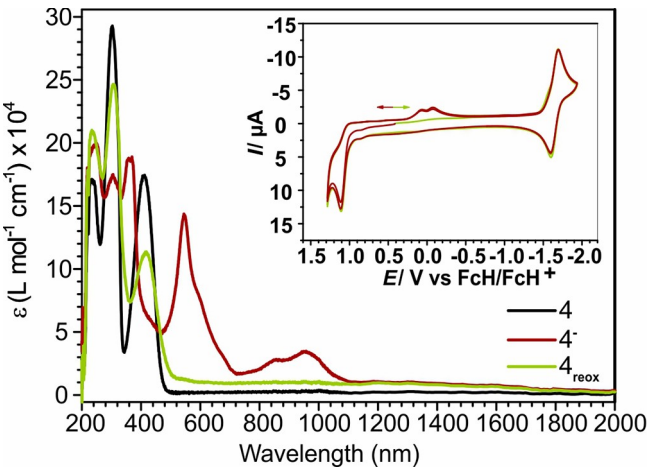

Figure 6. Absorption spectra of **4** (black), resulting species upon reduction (red) and after re-oxidation (green) of a $10^{<M->4}$M solution of DCM. The initial spectrum is not completely regained, indicating the irreversibility of the process. Inset: Cyclic voltammogram of **4** measured from 1.4 V to −2.0 V in both directions, oxidative direction (red) and reductive direction first (green). The follow up process observed at 0 V is visible after running through the oxidation at 1.11 V indicating that the reacting species is generated on the oxidative side.

The double peak at around 0 V only appears after the first oxidation (Figure 6, inset, red line) and it does not appear starting from 0.3 V to the reductive side (Figure 6, inset, green line). The peaks also appear, if one cycles first through reduction and then oxidation, so these peaks are clearly caused by a product that forms after oxidation (Figure S18B and C).

In order to probe the chemical reversibility of the redox processes and the follow-up reactions, UV/Vis/NIR-spectroelectrochemistry was employed for **3** and **4** (Figure 7 and Figure S19–S20). This was done using optically transparent thin layer electrochemical cells (OTTLE) with defined starting concentrations of about 1×10^{-4} M of the respective compound.[41] The absorption bands of the radical anions $\mathbf{3}^-$ and $\mathbf{4}^-$ formed upon reduction of **3** and **4** cover the whole visible spectrum and extend to the NIR. The respective maxima are located at 503 nm and 544 nm for $\mathbf{3}^-$ and $\mathbf{4}^-$ and have molar extinction coefficients of 12,000 and 14,000 $M^{-1}cm^{-1}$, respectively (Figure 7 and Table S9). Species $\mathbf{3}^-$ features two absorption bands at about 800 nm with a molar extinction coefficient of about 3,000 $M^{-1}cm^{-1}$ (Figure 7A).

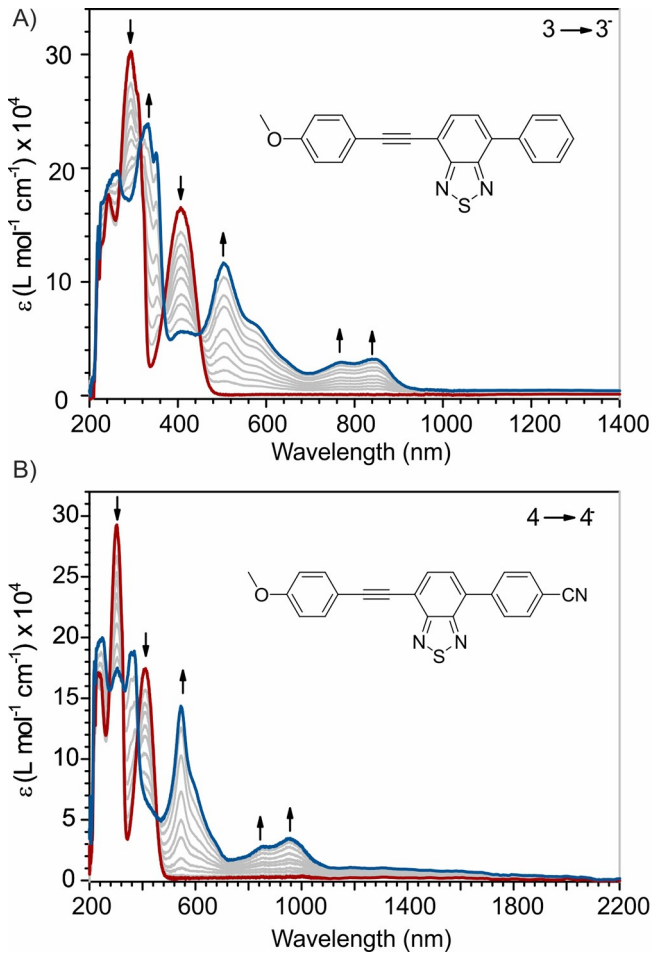

Figure 7. Absorption spectra of **3** (A) and **4** (B) before (red) and after first reduction (blue). Both show one pronounced maximum around 500 nm and a broad band absorption around 800–900 nm. The concentration was 10^{-4} M in DCM.

These absorption maxima are red-shifted to around 900 nm for species $\mathbf{4}^-$ and have comparable molar extinction coefficients. The absorption spectra of the re-oxidized compounds reveal that the reduction process is not completely reversible (Figure 6 and Figure S19/S20), since the absorption spectra of the respective neutral species after reduction are reduced relative to the initial spectra by about 25% and 35% for **3** and **4**, respectively. For **4**, the absorption spectrum may provide a hint for a possible polymerization (Figure 6). The oxidation of **3** leads to a decreased and slightly shifted absorption in the UV region at 307 nm with a molar extinction coefficient of about 18,000 $M^{-1}cm^{-1}$. Species $\mathbf{3}^+$ shows a broad absorption covering the complete Vis region extending up to 1,000 nm with molar extinction coefficients around 4,000 $M^{-1}cm^{-1}$ and a weak maximum at 566 nm. The irreversibility of this oxidation process is shown by the purple line and further proven by the absorption behavior after re-reduction highlighting a follow-up chemical reaction or decomposition of the compound (Figure S19). Since the oxidation processes of compounds **1**–**4** are very similar, only compound **3** was investigated exemplarily. As our spectroelectrochemical analysis of **3** and **4** showed irreversibility of the, seemingly reversible CV experiments, the characterization of **1** and **2** was omitted, owing to the higher reactivity already apparent in the cyclic voltammograms.

We presented a series of push-pull benzothiadiazole derivatives with photophysical properties governed by LE and ICT states that reveal fluorescence quantum yields (Φ_{fl}) of up to 98% in aprotic organic solvents of medium polarity and up to 60% in the polar protic ethanol. We succeeded in separating the effect of microenvironment polarity and viscosity on the optical properties of these dyes, thereby demonstrating a polarity-induced reduction in Φ_{fl} and fluorescence lifetime. The fact that the viscosity barely affects Φ_{fl} and the fluorescence decay kinetics suggests that a molecular motion like a rotation in the excited state is not involved in radiation-less deactivation of the excited states of the BDT dyes. Fluorescence studies of BDT crystals revealed still relatively high Φ_{fl} of 30%–70%. Spectroelectrochemical investigations showed broad absorption bands in the Vis/NIR for the reduced species. As demonstrated by CV experiments the first reduction step is at least partly reversible, in contrast to the second reduction step and the oxidation process. Although highly fluorescent BTDs with reversible electrochemical behavior are an attractive class of molecules for use as electrochemical switches, further research and more complex architectures will be necessary to stabilize charged BTD species.

Acknowledgements

We would like to acknowledge the assistance of the Core Facility BioSupraMol supported by the DFG.

Conflict of Interest

The authors declare no conflict of interest.

Keywords: absorption switching · benzothiadiazoles · fluorescence · redox switches · spectroelectrochemistry

[1] B. A. Da Silveira Neto, A. S. A. Lopes, G. Ebeling, R. S. Gonçalves, V. E. U. Costa, F. H. Quina, J. Dupont, *Tetrahedron* **2005**, *61*, 10975–10982.
[2] Z. Wang, Z. Peng, K. Huang, P. Lu, Y. Wang, *J. Mater. Chem. C* **2019**, *7*, 6706–6713.
[3] A. M. Thooft, K. Cassaidy, B. VanVeller, *J. Org. Chem.* **2017**, *82*, 8842–8847.
[4] Z. Peng, Z. Wang, Z. Huang, S. Liu, P. Lu, Y. Wang, *J. Mater. Chem. C* **2018**, *6*, 7864–7873.
[5] M. E. Mohanty, C. Madhu, V. L. Reddy, M. Paramasivam, P. R. Bangal, V. J. Rao, *Phys. Chem. Chem. Phys.* **2017**, *19*, 9118–9127.
[6] M. D'Alessandro, A. Amadei, I. Daidone, R. Po', A. Alessi, M. Aschi, *J. Phys. Chem. C* **2013**, *117*, 13785–13797.
[7] L. E. Polander, L. Pandey, S. Barlow, S. P. Tiwari, C. Risko, B. Kippelen, J.-L. Brédas, S. R. Marder, *J. Phys. Chem. C* **2011**, *115*, 23149–23163.
[8] C.-Y. Mei, L. Liang, F.-G. Zhao, J.-T. Wang, L.-F. Yu, Y.-X. Li, W.-S. Li, *Macromolecules* **2013**, *46*, 7920–7931.
[9] P. Ledwon, N. Thomson, E. Angioni, N. J. Findlay, P. J. Skabara, W. Domagala, *RSC Adv.* **2015**, *5*, 77303–77315.
[10] M. J. McAllister, J.-L. Li, D. H. Adamson, H. C. Schniepp, A. A. Abdala, J. Liu, M. Herrera-Alonso, D. L. Milius, R. Car, R. K. Prud'homme, I. A. Aksay, *Chem. Mater.* **2007**, *19*, 4396–4404.
[11] K. Shen, Z. Ju, L. Qin, T. Wang, H. Zheng, *Dyes Pigm.* **2017**, *136*, 515–521.
[12] S. S. M. Fernandes, A. Pereira, D. Ivanou, A. Mendes, M. M. M. Raposo, *Dyes Pigm.* **2018**, *151*, 89–94.
[13] M. Akhtaruzzaman, N. Kamata, J. Nishida, S. Ando, H. Tada, M. Tomura, Y. Yamashita, *Chem. Commun.* **2005**, 3183–3185.
[14] F. S. Mancilha, B. A. DaSilveira Neto, A. S. Lopes, P. F. Moreira, F. H. Quina, R. S. Gonçalves, J. Dupont, *Eur. J. Org. Chem.* **2006**, *2006*, 4924–4933.
[15] P. Rietsch, F. Witte, S. Sobottka, G. Germer, A. Becker, A. Guttler, B. Sarkar, B. Paulus, U. Resch-Genger, S. Eigler, *Angew. Chem. Int. Ed.* **2019**, *58*, 8235–8239.
[16] M. Shen, J. Rodriguez-Lopez, J. Huang, Q. Liu, X. H. Zhu, A. J. Bard, *J. Am. Chem. Soc.* **2010**, *132*, 13453–13461.
[17] R. S. Sánchez, R. Gras-Charles, J. L. Bourdelande, G. Guirado, J. Hernando, *J. Phys. Chem. C* **2012**, *116*, 7164–7172.
[18] H. V. Schroder, H. Hupatz, A. J. Achazi, S. Sobottka, B. Sarkar, B. Paulus, C. A. Schalley, *Chem. Eur. J.* **2017**, *23*, 2960–2967.
[19] Q. Chen, J. Sun, P. Li, I. Hod, P. Z. Moghadam, Z. S. Kean, R. Q. Snurr, J. T. Hupp, O. K. Farha, J. F. Stoddart, *J. Am. Chem. Soc.* **2016**, *138*, 14242–14245.
[20] C. M. Dickie, A. L. Laughlin, J. D. Wofford, N. S. Bhuvanesh, M. Nippe, *Chem. Sci.* **2017**, *8*, 8039–8049.
[21] M. Wałęsa-Chorab, M.-H. Tremblay, M. Ettaoussi, W. G. Skene, *Pure Appl. Chem.* **2015**, *87*, 649–661.
[22] P. Ledwon, P. Zassowski, T. Jarosz, M. Lapkowski, P. Wagner, V. Cherpak, P. Stakhira, *J. Mater. Chem. C* **2016**, *4*, 2219–2227.
[23] K.-W. Park, L. A. Serrano, S. Ahn, M. H. Baek, A. A. Wiles, G. Cooke, J. Hong, *Tetrahedron* **2017**, *73*, 1098–1104.
[24] C. Reichardt, *Chem. Rev.* **1994**, *94*, 2319–2358.
[25] D. Gudeika, A. Miasojedovas, O. Bezvikonnyi, D. Volyniuk, A. Gruodis, S. Jursenas, J. V. Grazulevicius, *Dyes Pigm.* **2019**, *166*, 217–225.
[26] P. C. Rodrigues, L. S. Berlim, D. Azevedo, N. C. Saavedra, P. N. Prasad, W. H. Schreiner, T. D. Atvars, L. Akcelrud, *J. Phys. Chem. A* **2012**, *116*, 3681–3690.
[27] J. R. Lakowicz, *Principles of Fluorescence Spectroscopy*, **2006**.
[28] N. Mataga, Y. Kaifu, M. Koizumi, *Bull. Chem. Soc. Jpn.* **1955**, *28*, 690–691.
[29] E. Lippert, *Z. Elektrochem.* **1957**, *61*, 962–975.
[30] J. Pina, J. S. de Melo, D. Breusov, U. Scherf, *Phys. Chem. Chem. Phys.* **2013**, *15*, 15204–15213.
[31] A. R. Harifi-Mood, M. Abbasi, *J. Solution Chem.* **2018**, *47*, 1503–1513.
[32] B. Y. Zaslavsky, L. M. Miheeva, E. A. Masimov, S. F. Djafarov, C. Reichardt, *J. Chem. Soc. Faraday Trans.* **1990**, *86*, 519–524.
[33] C. Hadad, S. Achelle, J. C. Garcia-Martinez, J. Rodriguez-Lopez, *J. Org. Chem.* **2011**, *76*, 3837–3845.
[34] M. N. Paddon-Row, A. M. Oliver, J. M. Warman, K. J. Smit, M. P. De Haas, H. Oevering, J. W. Verhoeven, *J. Phys. Chem.* **1988**, *92*, 6958–6962.
[35] N. Scholz, A. Jadhav, M. Shreykar, T. Behnke, N. Nirmalananthan, U. Resch-Genger, N. Sekar, *J. Fluoresc.* **2017**, *27*, 1949–1956.
[36] R. M. Yusop, A. Unciti-Broceta, M. Bradley, *Bioorg. Med. Chem. Lett.* **2012**, *22*, 5780–5783.
[37] C.-Y. Yu, C.-C. Hsu, H.-C. Weng, *RSC Adv.* **2018**, *8*, 12619–12627.
[38] C. Reichardt, *Chem. Rev.* **1994**, *94*, 2319–2358.
[39] M. Prashad, Y. Liu, O. Repič, *Tetrahedron Lett.* **2001**, *42*, 2277–2279.
[40] G. M. Martins, B. Shirinfar, T. Hardwick, A. Murtaza, N. Ahmed, *Catal. Sci. Technol.* **2019**, *9*, 5868–5881.
[41] S. R. Domingos, H. Luyten, F. van Anrooij, H. J. Sanders, B. H. Bakker, W. J. Buma, F. Hartl, S. Woutersen, *Rev. Sci. Instrum.* **2013**, *84*, 033103.

Manuscript received: June 4, 2020
Revised manuscript received: April 27, 2020
Accepted manuscript online: April 29, 2020
Version of record online: June 17, 2020